Dual-Affinity Re-Targeting proteins direct T cell–mediated cytolysis of latently HIV-infected cells

Julia A.M. Sung, … , David M. Margolis, Guido Ferrari

Research Article   AIDS/HIV

Enhancement of HIV-specific immunity is likely required to eliminate latent HIV infection. Here, we have developed an immunotherapeutic modality aimed to improve T cell–mediated clearance of HIV-1–infected cells. Specifically, we employed Dual-Affinity Re-Targeting (DART) proteins, which are bispecific, antibody-based molecules that can bind 2 distinct cell-surface molecules simultaneously. We designed DARTs with a monovalent HIV-1 envelope-binding (Env-binding) arm that was derived from broadly binding, antibody-dependent cellular cytotoxicity–mediating antibodies known to bind to HIV-infected target cells coupled to a monovalent CD3 binding arm designed to engage cytolytic effector T cells (referred to as HIVxCD3 DARTs). Thus, these DARTs redirected polyclonal T cells to specifically engage with and kill Env-expressing cells, including CD4+ T cells infected with different HIV-1 subtypes, thereby obviating the requirement for HIV-specific immunity. Using lymphocytes from patients on suppressive antiretroviral therapy (ART), we demonstrated that DARTs mediate CD8+ T cell clearance of CD4+ T cells that are superinfected with the HIV-1 strain JR-CSF or infected with autologous reservoir viruses isolated from HIV-infected–patient resting CD4+ T cells. Moreover, DARTs mediated CD8+ T cell clearance of HIV from resting CD4+ T cell cultures following induction of latent virus expression. Combined with HIV latency reversing agents, HIVxCD3 DARTs have the potential to be effective immunotherapeutic agents to clear latent HIV-1 reservoirs in HIV-infected individuals.

Find the latest version:

https://jci.me/82314/pdf

Dual-Affinity Re-Targeting proteins direct T cell–mediated cytolysis of latently HIV-infected cells

Julia A.M. Sung,[1] Joy Pickeral,[2] Liqin Liu,[3] Sherry A. Stanfield-Oakley,[2] Chia-Ying Kao Lam,[3] Carolina Garrido,[1] Justin Pollara,[2] Celia LaBranche,[2] Mattia Bonsignori,[4,5] M. Anthony Moody,[5,6] Yinhua Yang,[3] Robert Parks,[5] Nancie Archin,[1] Brigitte Allard,[1] Jennifer Kirchherr,[1] JoAnn D. Kuruc,[1] Cynthia L. Gay,[1] Myron S. Cohen,[1] Christina Ochsenbauer,[7] Kelly Soderberg,[5] Hua-Xin Liao,[4,5] David Montefiori,[2,5] Paul Moore,[3] Syd Johnson,[3] Scott Koenig,[3] Barton F. Haynes,[4,5] Jeffrey L. Nordstrom,[3] David M. Margolis,[1] and Guido Ferrari[2,5]

[1]Department of Medicine, University of North Carolina at Chapel Hill, Chapel Hill, North Carolina, USA. [2]Department of Surgery, Duke University, Durham, North Carolina, USA. [3]MacroGenics, Inc., Rockville, Maryland, USA. [4]Department of Medicine, Duke University, Durham, North Carolina, USA. [5]Duke Human Vaccine Institute, Duke University Medical Center, Durham, North Carolina, USA. [6]Department of Pediatrics, Duke University, Durham, North Carolina, USA. [7]Division of Hematology and Oncology, University of Alabama-Birmingham, Birmingham, Alabama, USA.

Enhancement of HIV-specific immunity is likely required to eliminate latent HIV infection. Here, we have developed an immunotherapeutic modality aimed to improve T cell–mediated clearance of HIV-1–infected cells. Specifically, we employed Dual-Affinity Re-Targeting (DART) proteins, which are bispecific, antibody-based molecules that can bind 2 distinct cell-surface molecules simultaneously. We designed DARTs with a monovalent HIV-1 envelope-binding (Env-binding) arm that was derived from broadly binding, antibody-dependent cellular cytotoxicity–mediating antibodies known to bind to HIV-infected target cells coupled to a monovalent CD3 binding arm designed to engage cytolytic effector T cells (referred to as HIVxCD3 DARTs). Thus, these DARTs redirected polyclonal T cells to specifically engage with and kill Env-expressing cells, including CD4+ T cells infected with different HIV-1 subtypes, thereby obviating the requirement for HIV-specific immunity. Using lymphocytes from patients on suppressive antiretroviral therapy (ART), we demonstrated that DARTs mediate CD8+ T cell clearance of CD4+ T cells that are superinfected with the HIV-1 strain JR-CSF or infected with autologous reservoir viruses isolated from HIV-infected–patient resting CD4+ T cells. Moreover, DARTs mediated CD8+ T cell clearance of HIV from resting CD4+ T cell cultures following induction of latent virus expression. Combined with HIV latency reversing agents, HIVxCD3 DARTs have the potential to be effective immunotherapeutic agents to clear latent HIV-1 reservoirs in HIV-infected individuals.

Introduction

The inability of antiretroviral therapy (ART) to eradicate HIV was first suggested by the demonstration of latent infection of resting CD4+ T cells (1) and then by the recovery of rare, integrated, replication-competent HIV from the resting CD4+ memory T cells of patients receiving potent ART (2–4). Current ART cannot eradicate HIV infection because these long-lived CD4+ T cells remain persistently infected and unrecognized by the immune system, with minimal expression of HIV genes or proteins (1, 5, 6). The persistence of quiescent HIV infection, primarily within central memory T cells, is a major obstacle to eradication of HIV infection (2–4, 7–9).

Viral persistence is also manifest in a substantial proportion of treated patients by very low levels of detectable viral RNA (10, 11) that represents expression of viral particles without effective rounds of new replication and does not appear to lead to drug resistance or failure of therapy (12, 13). However, persistent viremia demonstrates an inability of the immune response to recognize and clear HIV-1–infected cells.

Chronically infected individuals generally have rapid viral rebound when ART is withdrawn (14–16). This observation has suggested that the immune system in patients cannot control viremia, unless bolstered by a further intervention. Therapeutic immunization, even in individuals who initiated ART when CD4+ and CD8+ cellular immune responses remain relatively preserved, has thus far been unsuccessful in inducing enhanced anti-HIV immunity that can restrict viremia in the absence of ART (17). Therefore, eliminating the latent pool of HIV-infected cells that persist despite ART, as well as the unknown cells that are the source of low-level viremia found in most patients despite ART, requires new and innovative strategies. One initial step, the
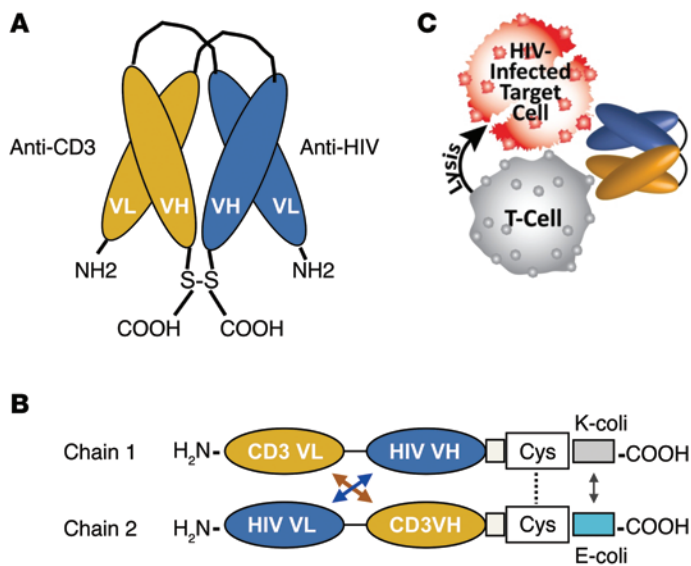
Figure 1. HIVxCD3 DART structure. (**A** and **B**) These DART molecules contain an anti–HIV-1 binding arm (A32 or 7B2) combined with an anti-CD3 binding arm (hXR32). They are composed of 2 polypeptide chains: one with the VL of anti-CD3 linked to the VH of anti-HIV; the second with the VL of anti-HIV linked to the VH of anti-CD3. The carboxy termini of the chains have an interchain disulfide bond and paired oppositely charged E-coil/K-coil dimerization domains. Control DARTs have one of the arms replaced by an irrelevant one derived from an anti-FITC antibody (4420) or from an anti-RSV antibody, palivizumab (RSV) sequence. (**C**) Schematic representation of HIVxCD3 DART binding to 2 distinct antigens simultaneously and redirecting the cytotoxic T cells (effectors) to lyse the Env-expressing, HIV-1–infected cells (targets).

disruption of latency and the induction of viral antigen expression in cells that are latently infected, is under intensive investigation (18, 19). However, as early progress is made in the development of latency reversing agents (LRAs), improvements in the ability to clear persistent infection must be sought, as well.

Latently infected cells are very rare, and even if the latent reservoir is as much as 60 times larger than the typical estimates of about 1 infected cell per 10^6 resting central memory CD4$^+$ cells (20), current LRAs might induce proviral transcription in only a fraction of this population, and the quantity of viral antigen presented might be low (21, 22). Therefore, a novel and robust immune response may be necessary to detect and clear both cells producing low-level viremia and in quiescently infected cells after inducing HIV-1 to leave the latent state.

Following the reactivation of latent HIV, viral antigens are presented on the surface of the cell and thus could be targeted by antibodies or antibody-derived molecules. Proof of concept for this approach has been provided by immunotoxins — bifunctional chimeric proteins consisting of a targeting domain, such as an antibody or a ligand, joined to a toxin effector domain (23). Although initial clinical trials using immunotoxins in HIV-infected individuals failed to have sustained impact on immunological or clinical markers (24), immunotoxin 3B3-PE38 (25) has been reported to reduce levels of HIV-infected cells that persist despite ART in the BLT humanized mouse model (26).

Several mAbs have been reported as capable of recognizing HIV-1–infected cells and engaging Fc-γ receptor–bearing cells to mediate antibody-dependent cellular cytotoxicity (ADCC) (27), such as A32 and 7B2, nonneutralizing mAbs that bind to conserved residues in gp120 (28) and gp41 (29, 30), respectively. Based on these properties, 2 Dual-Affinity Re-Targeting proteins (DART proteins) (31, 32) were generated in which HIV envelope targeting (Env-targeting) arms derived from the A32 and 7B2 mAbs were combined with a CD3 effector arm derived from hXR32, a humanized anti-CD3ε mAb, to generate 2 HIVxCD3 DARTs: A32xCD3 and 7B2xCD3 (Figure 1).

Bispecific molecules that coengage T cells with antigen-expressing target cells, such as DARTs and bispecific T cell engager

proteins (BiTEs), have been characterized and developed largely for use in oncology (31–34). They are dependent on the engagement of both of the binding arms to activate and redirect the cytolytic activity of polyclonal T cells, in a major histocompatibility complex–independent (MHC-independent) manner, against the antigen-expressing target cells (31–34). This class of bispecific molecules is effective in vivo at doses many-fold lower than those typically employed for mAbs (33, 34) and has been shown to be clinically potent and efficacious with acceptable safety, as evidenced by the approval of blinatumomab, a CD19xCD3 BiTE, for the treatment of relapsed or refractory B-precursor acute lymphoblastic leukemia (ALL) (35, 36). DARTs, which have interchain disulfide bonds at their C-termini and are structurally compact, making them well suited for forming stable cell-to-cell contacts between target and effector cells, exhibit greater potency than BiTEs in side-by-side comparisons (32, 37).

Herein, we demonstrate the ability of HIVxCD3 DARTs to redirect CD8$^+$ T cells against CD4$^+$ cells infected by HIV-1, including ones infected with authentic latent virus isolates emerging from HIV-infected patients' cells in model systems designed to mimic potential clinical HIV eradication strategies. The ability of HIVxCD3 DARTs to recognize conserved HIV-1 antigens on infected cells and simultaneously engage receptors on the membrane of polyclonal effector T cells will overcome the need to activate preexisting HIV-specific cytotoxic effector cells (38), thus surmounting a crucial hurdle that impedes the effective elimination of the reservoir of infected CD4$^+$ T cells.

Results

HIV arm selection for DARTs. A32 mAb binds to a conformational, CD4-inducible epitope in gp120 C1/C2 (within epitope cluster A) (28, 39–41), and 7B2 mAb binds to a linear epitope in gp41 cluster I (29, 30, 42). We tested these 2 mAbs for their ability to mediate ADCC against a panel of 22 representative HIV-1 infectious molecular clones (IMCs) of subtypes A, AE, B, and C (Supplemental Table 1; supplemental material available online with this article; doi:10.1172/JCI82314DS1). The A32 mAb recognized 21 (95%)
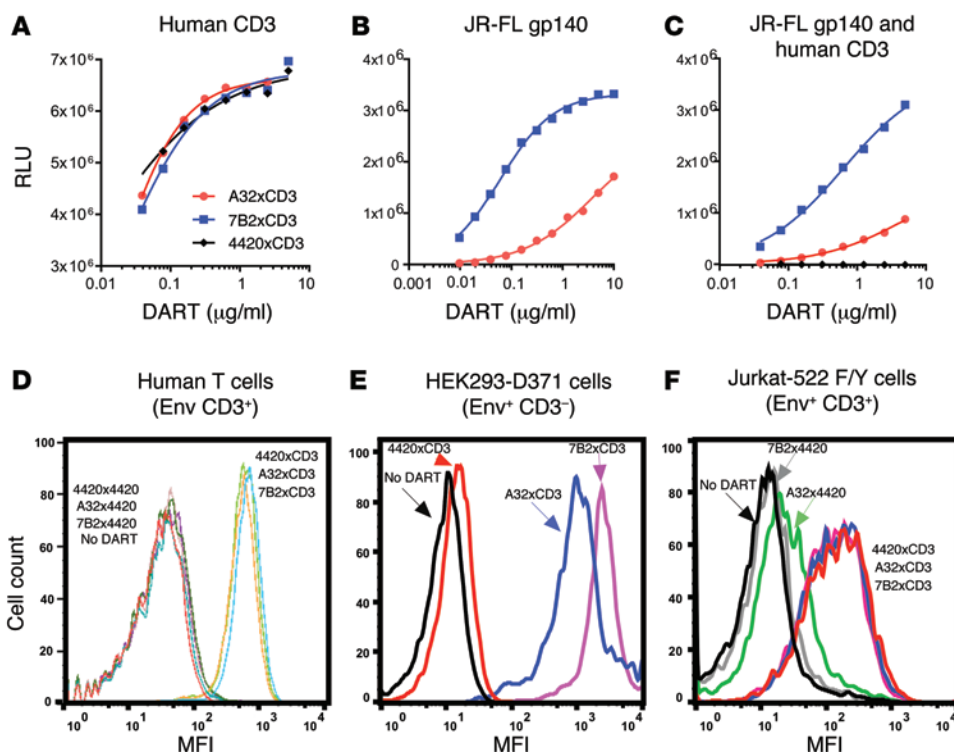
Figure 2. HIVxCD3 DART binding properties. (**A**–**C**) Antigen binding by ELISA. DART binding to human CD3 protein (**A**), to JR-FL gp140 protein (**B**), or simultaneously to both JR-FL gp140 and human CD3 proteins (**C**). (**D**–**F**) Cell-surface binding by flow cytometry analysis. DART binding to primary human T cells expressing CD3 (**D**); to HEK293-D371 cells expressing HIV-1 Env, CM244, subtype AE (**E**); or to Jurkat-522 F/Y cells expressing CD3 and HIV-1 Env, HXBC2, subtype B (**F**). Data are reported as mean fluorescence intensity (MFI). CD3 and Env expression characteristics of the cells are reported in parenthesis. A32 and 7B2 are targeting arms that recognize HIV-1 gp120 and gp41, respectively; CD3 is the effector arm that recognizes CD3ε; and hBU12, RSV, and 4420 are irrelevant, negative control arms.

of the HIV-1 IMCs with an average percent specific lysis (%SL) of 43.69% (range 12%–86%; Supplemental Figure 1). The 7B2 mAb recognized 20 (91%) of the HIV-1 IMCs with an average %SL of 39.58% (range 15%–74%; Supplemental Figure 1). In addition to possessing breadth and efficiency in mediating ADCC — indicating epitope accessibility at the surface of HIV-infected cells, a necessary property for HIVxCD3 DARTs — the A32 and 7B2 mAbs are attractive sources for Env binding domains for DARTs, as the residues in Env that influence binding by these mAbs are highly conserved among all HIV-1 subtypes (Supplemental Figure 2). Based on these properties, 2 HIVxCD3 DARTs were generated in which HIV targeting arms derived from the A32 and 7B2 mAbs were combined with a CD3 effector arm derived from hXR32, a humanized anti-CD3ε mAb (Figure 1). These HIVxCD3 DARTs are named A32xCD3 and 7B2xCD3. Control DARTs with an irrelevant arm — derived from an anti-FITC antibody (4420) or from palivizumab, an antibody to the respiratory syncytial virus (RSV) fusion protein antibody — instead of the HIV arm (4420xCD3, RSVxCD3) or CD3 arm (A32x4420, 7B2x4420) were also generated.

HIV DART binding properties. A32xCD3 and 7B2xCD3 each exhibited binding to recombinant human CD3 and HIV-1 Env proteins, individually and simultaneously, as shown by ELISA (Figure 2, A–C). While the binding to CD3 protein was similar for both DARTs, the magnitude of binding to JR-FL gp140 CF was greater for 7B2xCD3 than for A32xCD3, likely due to the fact that the conformational A32 epitope is highly CD4 dependent (41–44). Based on surface plasmon resonance (SPR), the equilibrium dissociation constants (K_D) for CD3 arm binding were 3.6 nM and 6.1 nM for A32xCD3 and 7B2xCD3, respectively; K_D for HIV arm binding was 47.7 nM for A32xCD3 using M.ConS gp140 CFI, and 15.1 nM for 7B2xCD3 using JR-FL gp140 CF, respectively (Supplemental

Table 2). Different Env proteins were utilized for these 2 DARTs in the SPR studies because A32xCD3 binding to JR-FL gp140 CF was inefficient and 7B2xCD3 binding to M.ConS gp140 CFI, due to its lack of the gp41 cluster I sequence, was precluded.

HIVxCD3 DARTs bind to their cell-surface antigens with specificity. DARTs with CD3 effector arms (A32xCD3, 7B2xCD3, 4420xCD3) bind to human CD3+ T cells with similar efficiencies, whereas DARTs with the CD3 arm replaced by an irrelevant arm (A32x4420, 7B2x4420) or with 2 irrelevant arms (hBU12x4420) do not bind (Figure 2D). HIVxCD3 DARTs (A32xCD3, 7B2xCD3) bind efficiently to HEK293-D371 cells that express subtype AE CM244 Env (Figure 2E), and similar binding activity is observed with the A32x4420 and 7B2x4420 control DARTs (Supplemental Figure 3). As expected, the RSVxCD3 control DART does not bind to these cells (Figure 2E). A32xCD3 and 7B2xCD3 bind to Jurkat-522 F/Y cells, which express both CD3 and subtype B HXBc2 Env (45), and binding via the CD3 arm predominates as shown by the equivalence of 4420xCD3, A32xCD3, and 7B2xCD3 binding. When the CD3 arm is replaced by the irrelevant 4420 arm to ablate CD3 binding, low-level binding to the cell-surface Env is detected with A32x4420, but not with 7B2x4420 (Figure 2F).

HIVxCD3 DART–redirected T cell killing of Env-expressing cell lines and concomitant T cell activation. Jurkat-522 F/Y is a human CD4+ cell line that expresses *env* and serves as a model for HIV-infected CD4+ T cells, and Jurkat-ΔKS is a control cell line that is identical, except for a deletion/frameshift mutation in the *env* gene that precludes its expression (45). These cell lines were utilized to evaluate the ability of HIVxCD3 DARTs to mediate redirected T cell killing of Env+ target cells. Target cell cytolysis was determined by measuring lactate dehydrogenase (LDH) release with our standard assay, and the results were confirmed by luminescence
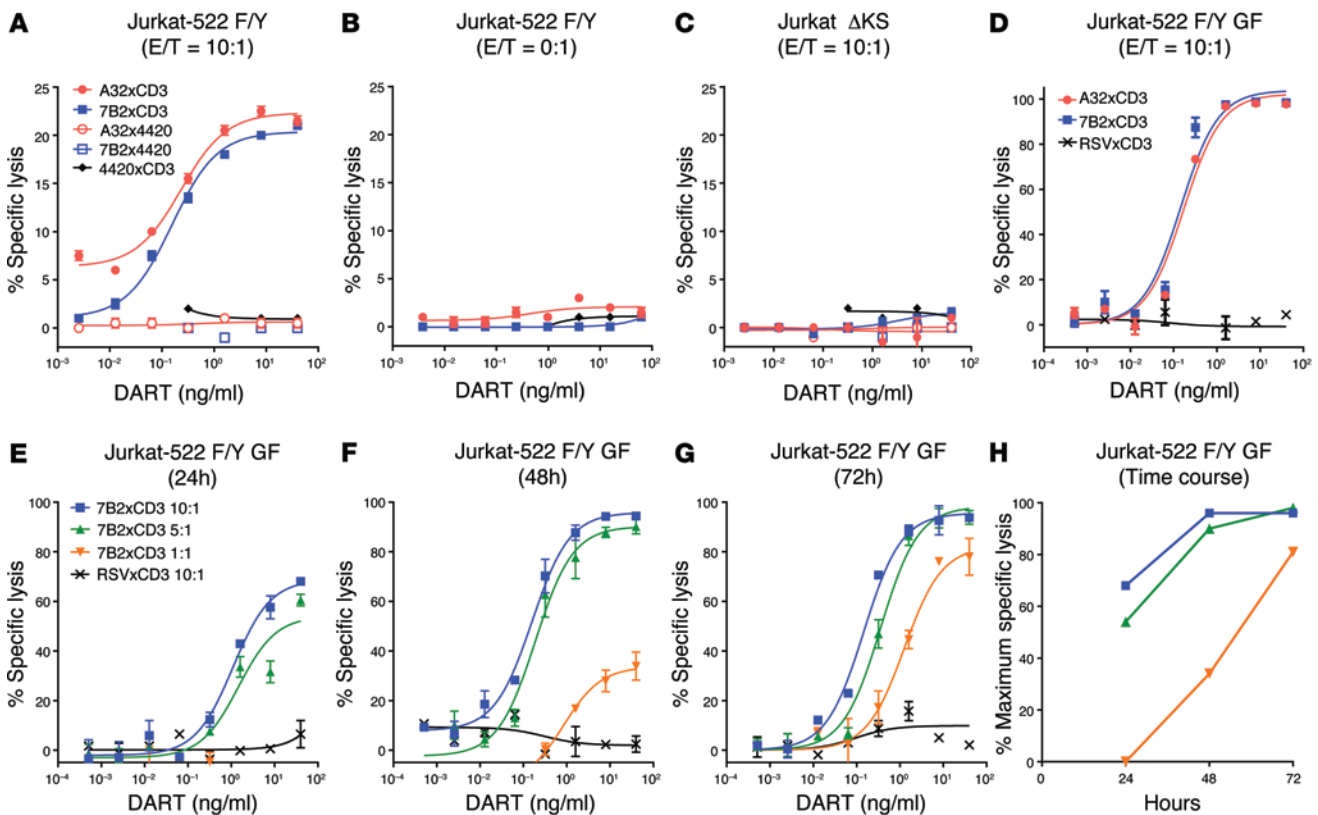
Figure 3. HIVxCD3 DART–redirected T cell killing of Env⁺ target cells. (**A**) DART concentration–dependent killing of Env⁺ Jurkat-522 F/Y cells in the presence of human T cells at an E/T ratio of 10:1 for 48 hours with cytolysis measured by LDH release assay; EC$_{50}$ values were 230 and 160 pg/ml for A32xCD3 and 7B2xCD3, respectively. The control DARTs (A32x4420, 7B2x4420, 4420xCD3) were inactive. (**B**) Lack of DART-mediated killing of Env⁺ Jurkat-522 F/Y cells in the absence of effector T cells with cytolysis measured by LDH release assay. (**C**) Lack of DART-redirected T cell killing of Env⁻ Jurkat ΔKS cells at an E/T ratio of 10:1 for 48 hours with cytolysis measured by LDH release assay. (**D**) DART concentration–dependent killing of Env⁺ Jurkat-522 F/Y GF cells in the presence of human T cells at an E/T ratio of 10:1 for 48 hours with cytolysis measured by LUM assay; EC$_{50}$ values were 172 and 147 pg/ml for A32xCD3 and 7B2xCD3, respectively. (**E–G**) 7B2xCD3 DART concentration–dependent redirected T cell killing of Env⁺ Jurkat-522 F/Y GF cells at different E/T ratios (10:1, 5:1, 1:1) and incubation times (24, 48, 72 hours) with cytolysis measured by LUM assay. (**H**) Time course of maximal cytolytic activity with 7B2xCD3 at different E/T ratios (data from **E–G**).

(LUM) assay. As measured by LDH release assays, A32xCD3 and 7B2xCD3 redirected human T cells derived from healthy donors to kill the Jurkat-522 F/Y cells in a concentration-dependent manner at an effector/target cell ratio (E/T ratio) of 10:1, and these 2 HIVx-DARTs exhibited similar potencies after 48 hours of incubation with 50% effective concentrations (EC$_{50}$) of 160–230 pg/ml (Figure 3A). No DART-mediated redirected T cell killing of Jurkat-522 F/Y cells occurred with control DARTs (4420xCD3, A32x4420, 7B2x4420) in which the HIV arm or CD3 arm was replaced by an irrelevant one (Figure 3A). The A32xCD3 and 7B2xCD3 DARTs did not mediate target-cell killing when the effector T cells were omitted (Figure 3B) or when the target cells lacked Env expression (Figure 3C). These data demonstrate a strict requirement for Env-expressing target cells and their coengagement with CD3-expressing effector cells for HIVxCD3 DART–mediated cytolytic activity.

As measured by LUM assays, A32xCD3 and 7B2xCD3 exhibited similar potencies for redirected T cell killing of Jurkat-522 F/Y GF cells with EC$_{50}$ values of 140–170 pg/ml (Figure 3D), which were close to those measured with the LDH release assay, indicating consistency across the 2 different assay modalities. Moreover, with the sensitivity and specificity of the LUM assay, DART-dependent elim-ination of the Env⁺ target cells was nearly complete (>98%), while the 4420xCD3 control DART mediated no cytotoxicity (Figure 3D). HIVxCD3 DART–redirected T cell–killing activity was time and E/T ratio dependent. Near complete cytolysis with 7B2xCD3 was reached at 48 hours at E/T ratios of 10:1 and 5:1, whereas high-level cytolysis (>80%) at an E/T ratio of 1:1 was delayed until 72 hours (Figure 3, E–H), suggesting that time is the limiting factor for the efficient elimination of target cells at lower E/T cell ratios.

Concomitant with redirecting T cell–killing activity, the HIVxCD3 DARTs induced T cell activation (measured by upregulation of the activation marker CD25) in the presence of the Env⁺ target cells, with CD25 upregulated in CD8⁺ T cells to a greater extent than in CD4⁺ T cells (Supplemental Figure 4). The overall data demonstrate that A32xCD3 and 7B2xCD3 potently activate and redirect T cells, especially CD8⁺ T cells, to specifically kill Env-expressing target cells. Moreover, the killing data confirm that both DARTs were capable of recognizing and binding to Env antigens on the surface of a CD4⁺ cell line, even though the detection of Env binding by FACS analysis was negligible (Figure 2F).

HIVxCD3 DARTs bind to the surface of HIV-1–infected CD4⁺ T cells and redirect CD8⁺ T cells to kill HIV-1–infected CD4⁺ cells
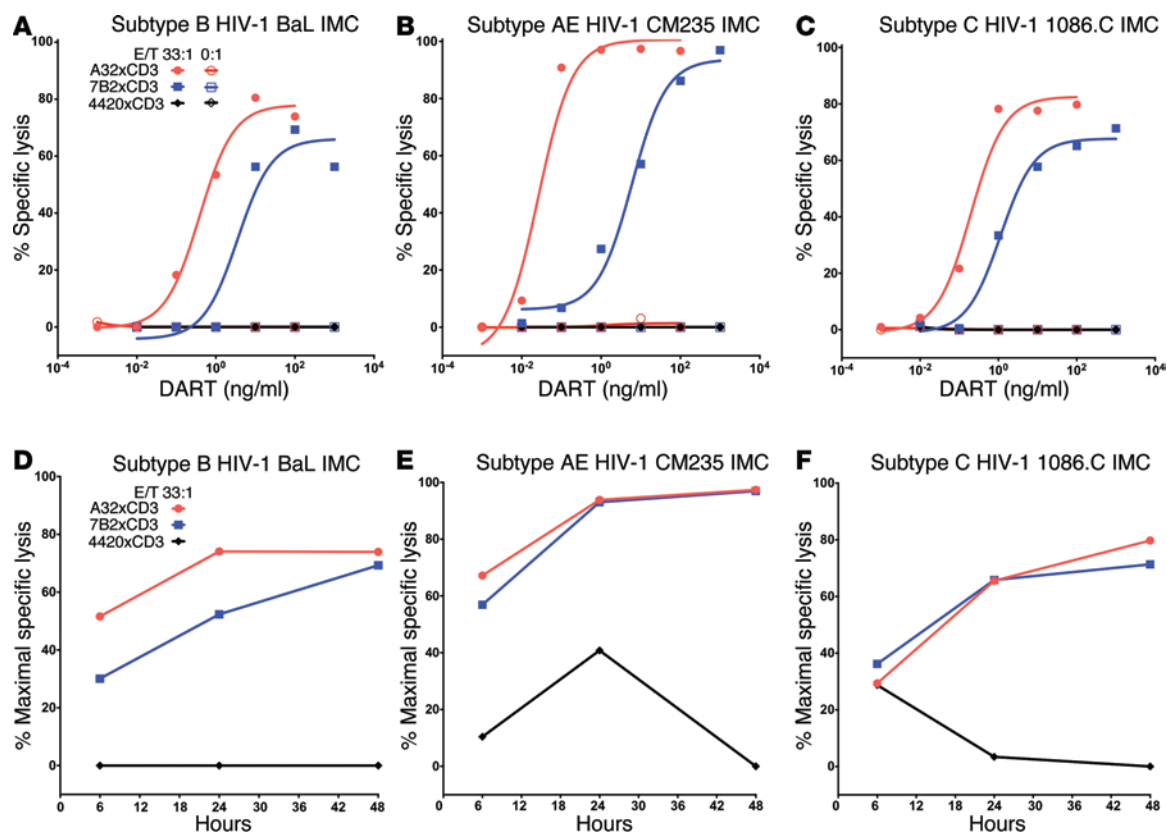
Figure 4. HIVxCD3 DARTs redirect T cell cytotoxicity against CD4+ cells infected with HIV-1 IMCs of different subtypes. (**A–C**) DART-concentration dependence. Activated CD4+ T cells from a HIV-1 seronegative donor were infected with HIV-1 subtype B BaL (**A**), subtype AE CM235 (**B**), or subtype C 1086.C (**C**) IMC and incubated for 48 hours with A32xCD3 (red circles), 7B2xCD3 (blue squares), or 4420xCD3 (black diamonds) in the presence of autologous resting CD8+ T cells at an E/T ratio of 33:1 (filled symbols) or in the absence of effector cells (E/T ratio of 0:1) (open symbols). The data are reported as %SL. DART concentrations ranged from 0.001–1,000 ng/ml. (**D–F**) Time course. The data represent the maximal %SL observed at 6, 24, and 48 hours for each DART against CD4+ T cells infected infected with HIV-1 subtype B BaL (**D**), subtype AE CM235 (**E**), or subtype C 1086.C (**F**) IMC and incubated with autologous resting CD8+ T cells at an E/T ratio of 33:1.

using lymphocytes from HIV-1 seronegative donors. We evaluated the A32x4420 and 7B2x4420 DARTs for their ability to bind and redirect the killing of CD4+ T cells infected with HIV-1 IMCs representing subtype AE CM235, subtype B BaL, and subtype C 1086.C HIV-1 isolates. Each IMC was engineered with a luciferase reporter gene to quantitatively measure the cytolysis of infected target cells. To assess binding to infected cell-surface Env, A32x4420 and 7B2x4420 DARTs (which lack CD3 effector arms) were compared with the parental A32 and 7B2 mAbs. We observed similar staining of the p24+ (infected) CD4+ T cells by both HIVxCD3 DARTs independently from the HIV-1 IMC used for the infection (Supplemental Figure 5). Interestingly, staining with the A32x4420 DART recapitulated closely the staining with the A32 mAbs; in contrast, the 7B2x4420 DART recognized >66% of the HIV-1–infected cells (range 66%–78%) compared with the >24% recognized by the 7B2 mAb (range 24%–38%), suggesting that the DART has a better accessibility to the cluster I gp41 epitope compared with the mAb (Supplemental Figure 5). The secondary conjugated antibodies and the palivizumab mAb utilized as controls recognized less than 5% HIV-1–infected CD4+ T cells.

We subsequently investigated the ability of A32xCD3 and 7B2xCD3 to redirect CD8+ T cells from HIV-1 seronegative donors

against autologous CD4+ T cells infected with the 3 HIV-1 IMCs. The 2 HIVxCD3 DARTs redirected autologous CD8+ T effector cells to kill subtype B BaL (Figure 4A), subtype AE CM235 (Figure 4B), and subtype C 1086.C (Figure 4C) IMC-infected CD4+ target cells in a concentration-dependent manner, whereas the control DART (4420xCD3) was inactive. The greater potency exhibited by A32xCD3 ($EC_{50} \leq 1$ ng/ml) compared with 7B2xCD3 (EC_{50} ~10 ng/ml) in these studies with IMC-infected CD4+ cells contrasts with the similar potencies observed in the studies with Env+ cell lines (Figure 3, A–C). DART-mediated killing of the IMC-infected CD4+ T cells was dependent on the presence of CD8+ effector cells, and no cytolytic activity was observed in their absence (Figure 4, A–C). In time-course studies, DART-dependent cytolytic activity was evident at 6 hours with maximal activity (>70% cytolysis) at 48 hours (Figure 4, D–F).

To gain insight into the frequency of effector T cells recruited by the DARTs to kill HIV-1–infected target cells, we assessed the ability of DARTs to induce degranulation of the CD8+ T cells obtained from 5 HIV-1 seronegative donors when coincubated with autologous HIV-1 BaL IMC-infected CD4+ cells under the same conditions used to detect cytolytic activity. The example of the gating strategy adopted for data analysis is illustrated in Figure 5,
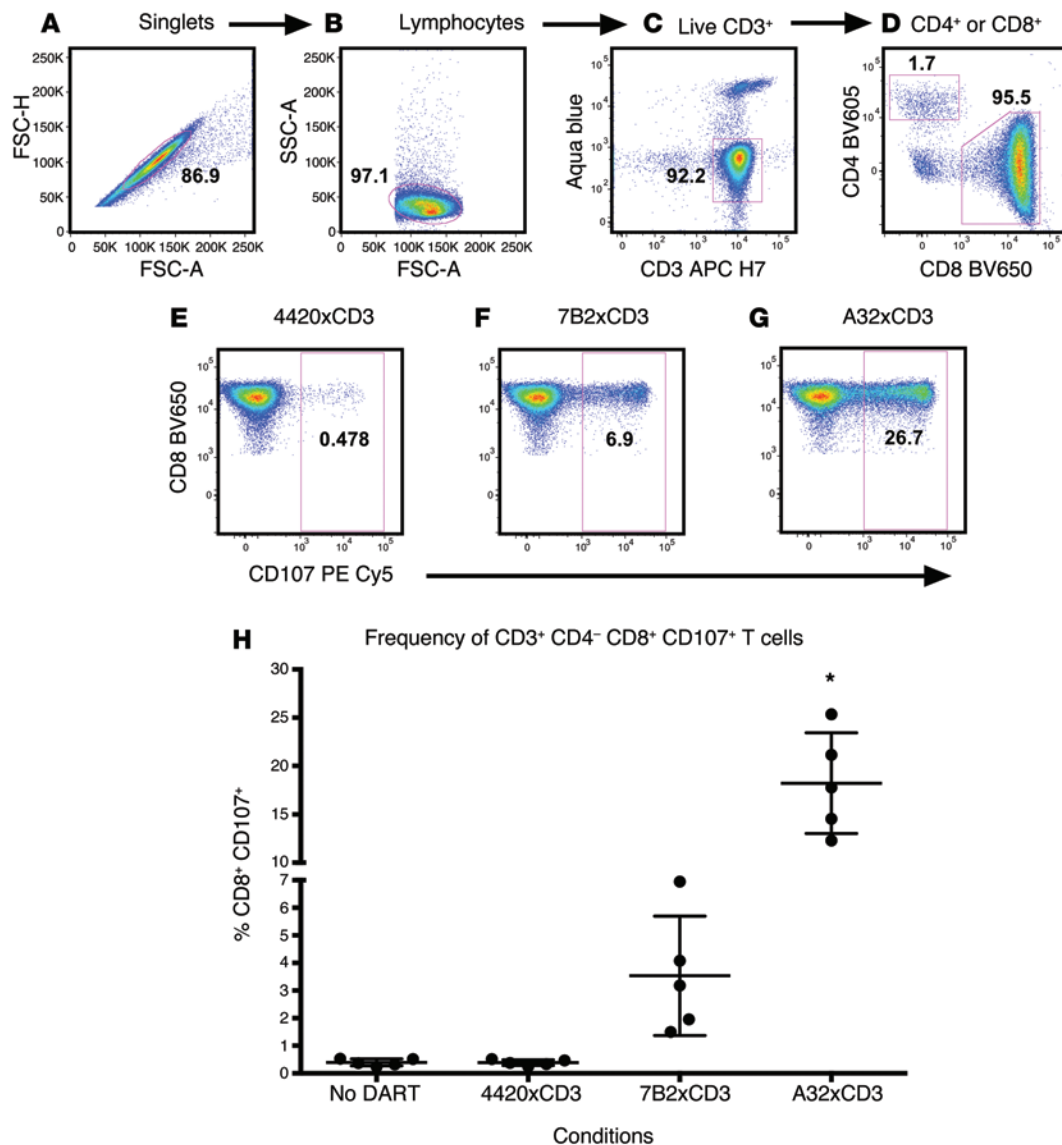
Figure 5. HIVxCD3 DARTs induce specific degranulation of CD8+ T cells. (A–D) Schematic of gating strategy to identify live/CD3+CD8+CD107+ T cells after their incubation with HIV-1 BaL–infected target cells in the presence of DARTs for 6 hours. **(E–G)** Dot plots represent the percentage of live/CD3+CD8+CD107+ cells observed in the presence of 1 ng/ml of 4420xCD3 **(E)**, 7B2xCD3 **(F)**, or A32xCD3 **(G)**. **(H)** Frequency of the CD3+CD4−CD8+CD107+ T cells observed in each of the 5 HIV-1 seronegative healthy donors after 6 hours of incubation with the autologous infected CD4+ T cells using the E/T ratio of 33:1. Each symbol represents the average of duplicate stimulations performed for each donor. The lines represent the mean ± SD. *$P < 0.05$ after Dunnett's test for multiple comparisons.

A–G. The mean frequency of live/CD3+/CD8+/CD107+ cells (Figure 5H) under control conditions (absence of HIVxCD3 DART or presence of control DART) was 0.38% (standard deviation 0.10%; range 0.24%–0.51%), which increased to an average 3.53% (range 1.5%–6.9%) or 18.23% (range 12.30%–23.35%) in the presence of 1 ng/ml 7B2xCD3 or A32xCD3, respectively. The data demonstrate that HIVxCD3 DARTs can specifically induce degranulation of resting CD8+ T cells in the presence of Env-expressing target cells (autologous HIV-1–infected CD4+ T cells).

HIVxCD3 DART–redirected CD8+ T cell–killing activity against JR-CSF–infected cells from seronegative donors. A viral clearance assay measuring HIV *gag* p24 antigen production was utilized as an alternative method to assess DART-redirected T cell–killing activity. CD4+ cells from healthy donors were superinfected with the

HIV-1 clade B clone JR-CSF and incubated with autologous CD8+ T cells at an E/T ratio of 1:1 in the absence or presence of 100 ng/ml DARTs for 7 days. In experiments with 2 different donors, addition of the control DART (4420xCD3) did not significantly reduce p24 production compared with incubations performed in the absence of DARTs, whereas addition of A32xCD3 or 7B2xCD3 significantly reduced p24 production to a similar extent (by 72%–96% or 87%–99%, respectively; $P < 0.05$ Dunnett's test for multiple comparisons; Figure 6, A and B). The viral clearance assay was also conducted in the presence of integrase and nonnucleoside reverse transcriptase inhibitors once infection was established, at the time of addition of effector cells and DARTs, to block further rounds of infection. When antiretrovirals (ARVs) were included in the assay, A32xCD3 and 7B2xCD3 still mediated a trend toward reduction
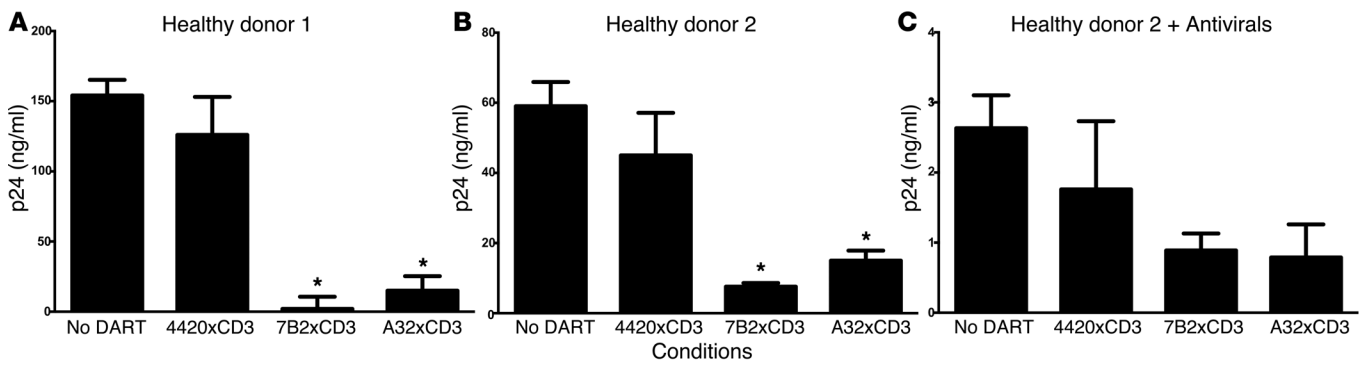
Figure 6. Viral clearance assay to assess HIVxCD3 DART redirected CD8+ T cell killing of autologous JR-CSF–infected CD4+ T cells from healthy HIV seronegative donors. Activated CD4+ T cells from HIV seronegative donors were infected with HIV-1 clone JR-CSF and then incubated with autologous resting CD8+ T effector cells at an E/T ratio of 1:1 in the absence (No DART) or presence of HIVxCD3 or control DARTs at a concentration of 100 ng/ml for 7 days. Results are shown for 2 healthy donors (**A** and **B**), as well as for healthy donor 2 in the presence of integrase and nonnucleoside reverse transcriptase inhibitors during the coculture period to inhibit virus replication (**C**). Each bar represents the absolute p24 concentration detected in culture supernatants. Error bars represent standard error mean (± SEM) of $n = 3$. *$P < 0.05$ with Dunnett's test for multiple comparisons.

in p24 production. This did not reach statistical significance, likely due to low levels of baseline p24 production with the ARVs (Figure 6C), suggesting that the DARTs are not acting by inhibition of virus spread but rather through clearance of infected cells.

HIVxCD3 DARTs redirect CD8+ T cells to clear JR-CSF–superinfected CD4+ cells using lymphocytes from patients on suppressive ART. Chronic ART is characterized by dysfunctional and exhausted T cell responses (46, 47) and thus confirmation of robust DART-mediated T cell–redirected clearance activity in patient samples ex vivo is critical. We therefore evaluated the activity of HIVxCD3 DARTs in viral clearance assays with lymphocytes from 8 HIV-infected individuals on suppressive ART. All participants were on ART for at least 6 months at the time of study with virus load <50 copies/ml but otherwise exhibited diverse clinical backgrounds (Supplemental Table 3).

Because T cells from HIV-1 seropositive subjects could be more susceptible to apoptosis than those from seronegative subjects (48), we first evaluated whether HIVxCD3 DARTs, in the absence of target cells, might impact T cell viability, which could confound the analysis of DART activity with patients' cells. Following 7 days of culture of either CD4+ or CD8+ T cells from HIV-infected, ART-suppressed patients in the presence of 100 ng/ml DART, which mimics the viral clearance assay conditions, we did not observe decreases in T cell viability based on Annexin V/7-amino-actinomycin D (7 AAD) staining (Supplemental Figure 6, A and B). Moreover, no changes in activation markers (HLA-DR, CD25) on unstimulated CD4+ or CD8+ T cells were observed after culture with HIVxCD3 or control DARTs (Supplemental Figure 6, C and D), suggesting that engagement of the CD3 arm alone does not activate patients' CD8+ or CD4+ T cells ex vivo.

Using the lymphocytes from 8 HIV-1–infected patients on suppressive ART, viral clearance assays were conducted in which CD4+ cells were superinfected with HIV-1 JR-CSF (target cells) and incubated with autologous CD8+ cells (effectors) at E/T ratios of 0:1, 1:10, or 1:1 in the absence or presence of 100 ng/ml DARTs for 7 days. HIVxCD3 DART activity occurred even in the absence of added CD8+ T cells, indicating that, under these experimental conditions, CD4+ T cells may be recruited as effector cells; compared with control, p24 production was reduced by 0.89 log with

7B2xCD3 ($P < 0.05$), by 0.32 log with A32xCD3 ($P =$ NS), and by 0.81 with a 1:1 cocktail of both DARTs ($P < 0.05$) (Figure 7A). Indeed, the addition of fully active DARTs led to significantly increased degranulation of CD4+ T cells when in the presence of infected target cells (Figure 7, G and H). The addition of CD8+ T cells as effectors resulted in further reductions in p24 levels; compared with the 0.13 log reduction seen with CD8+ T cells alone at an E/T of 1:10, p24 production was reduced by 1.2 log with 7B2xCD3 ($P < 0.05$), by 0.6 log with A32xCD3 ($P =$ NS), and by 1.8 log with a cocktail of the 2 DARTs ($P < 0.05$) (Figure 7B). Even more marked reductions were found with the higher E/T ratio of 1:1, where CD8+ T cells alone accounted for a 0.7 log reduction, but p24 production was reduced by 2.8 log with 7B2xCD3 ($P < 0.05$), by 1.6 log with A32xCD3 ($P =$ NS), and by 2.8 log with a cocktail of the 2 DARTs ($P < 0.05$) (Figure 7C). Significant reductions were seen even in the absence of any detectable baseline CD8+ T cell antiviral activity, and in 3 cases, no virus was able to be recovered following incubation with DARTs (patient 749 with both fully active DARTs, and patients 720 and 725 with 7B2xCD3). The absolute HIV *gag* p24 antigen values are provided in Supplemental Table 4.

HIVxCD3 DARTs redirect CD8+ T cells to clear autologous reservoir virus–superinfected CD4+ cells using lymphocytes from patients on suppressive ART. We evaluated the ability of the DARTs to redirect T cells against target cells expressing *env* sequences arising from the latent reservoir through the use of viral clearance assays employing autologous reservoir virus–infected (AR virus–infected) CD4+ target cells from 5 patients (Figure 7, D–F). Patient AR virus isolates were generated from pooled supernatants of limiting dilution cultures of mitogen-stimulated resting CD4+ T cells to reflect the diversity of virus that may be encountered in vivo following reactivation of latent virus. Despite the diversity of the AR virus isolates, DART activity mirrored that seen with JR-CSF–infected target cells. Modest activity was observed with AR-infected target cells in the absence of CD8+ effectors (thus attributed to CD4+ T cells; Figure 7D), with p24 production reduced by 0.32 log with 7B2xCD3 and by 0.20 log with A32xCD3 ($P =$ NS due to higher variance in response to 7B2xCD3) and by 0.51 log with a 1:1 cocktail of both DARTs ($P < 0.05$), whereas no activity was observed with
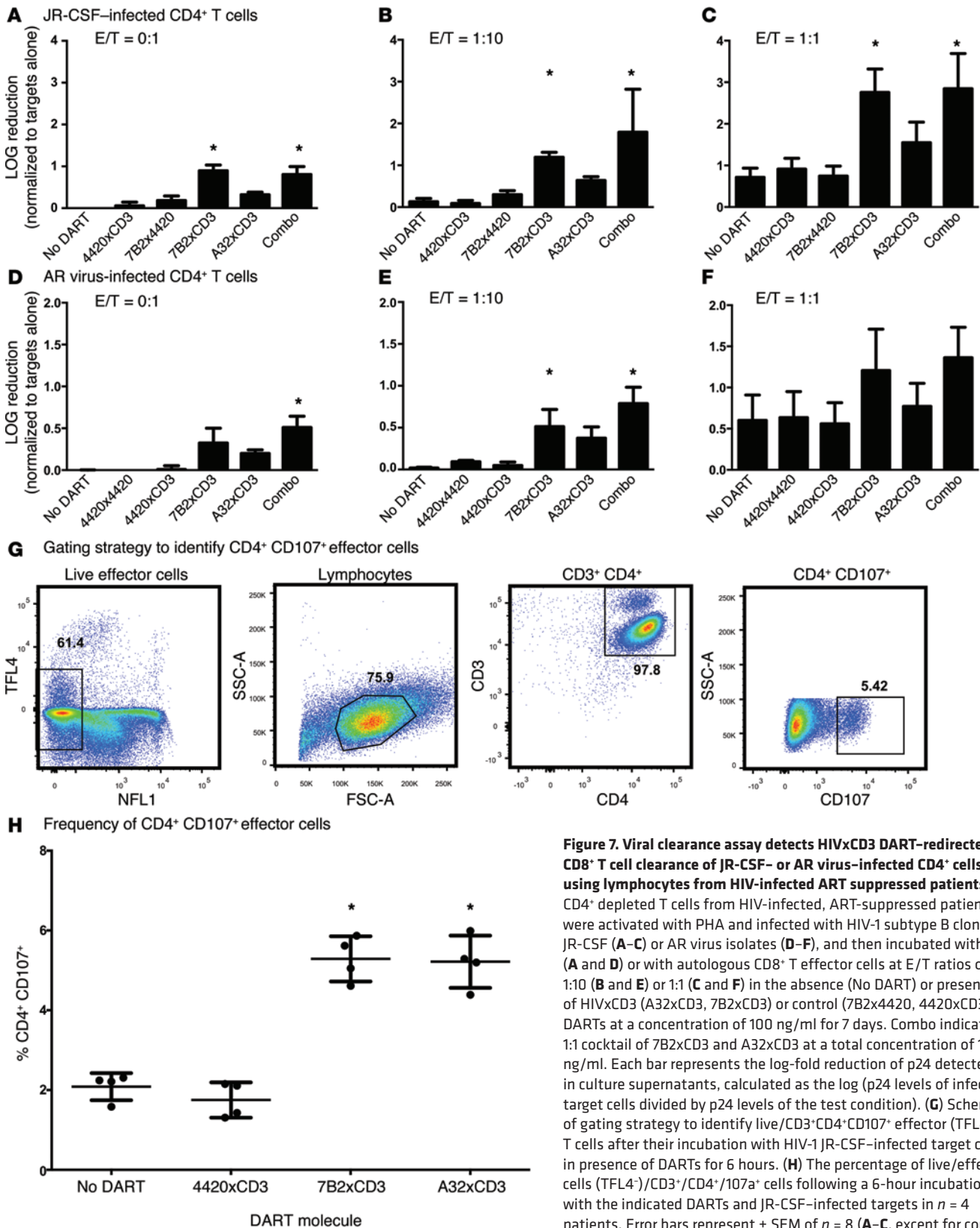
Figure 7. Viral clearance assay detects HIVxCD3 DART–redirected CD8+ T cell clearance of JR-CSF– or AR virus–infected CD4+ cells using lymphocytes from HIV-infected ART suppressed patients. CD4+ depleted T cells from HIV-infected, ART-suppressed patients were activated with PHA and infected with HIV-1 subtype B clone JR-CSF (A–C) or AR virus isolates (D–F), and then incubated without (A and D) or with autologous CD8+ T effector cells at E/T ratios of 1:10 (B and E) or 1:1 (C and F) in the absence (No DART) or presence of HIVxCD3 (A32xCD3, 7B2xCD3) or control (7B2x4420, 4420xCD3) DARTs at a concentration of 100 ng/ml for 7 days. Combo indicates a 1:1 cocktail of 7B2xCD3 and A32xCD3 at a total concentration of 100 ng/ml. Each bar represents the log-fold reduction of p24 detected in culture supernatants, calculated as the log (p24 levels of infected target cells divided by p24 levels of the test condition). (G) Schematic of gating strategy to identify live/CD3+CD4+CD107+ effector (TFL4−) T cells after their incubation with HIV-1 JR-CSF–infected target cells in presence of DARTs for 6 hours. (H) The percentage of live/effector cells (TFL4−)/CD3+/CD4+/107a+ cells following a 6-hour incubation with the indicated DARTs and JR-CSF–infected targets in n = 4 patients. Error bars represent ± SEM of n = 8 (A–C, except for combo [n = 5] and 7B2x4420 [n = 6]), n = 5 (D–F), and n = 4 (G and H). *P < 0.05 with Dunnett's test for multiple comparisons.
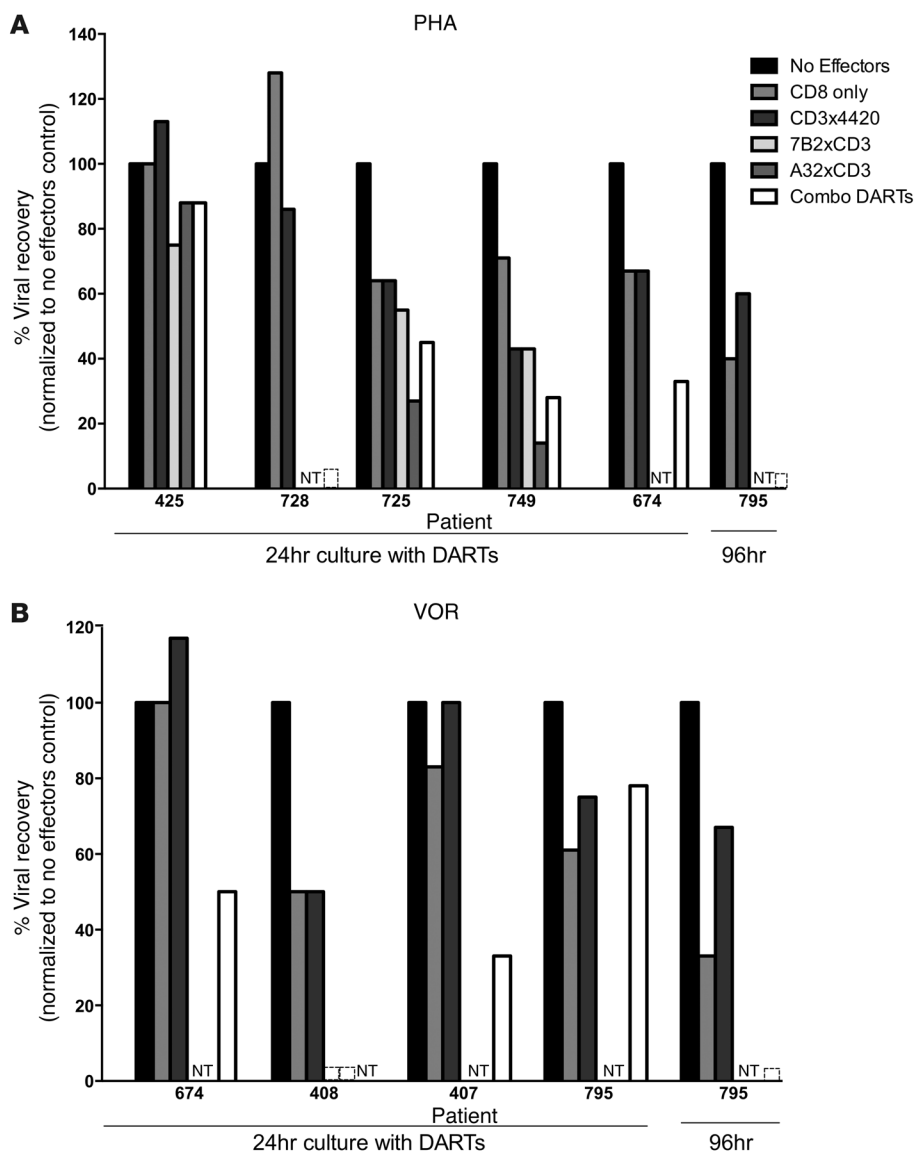
Figure 8. LCA to assess HIVxCD3 DART–redirected CD8+ T cell activity. Resting CD4+ T cells from HIV-infected, ART-suppressed patients were incubated with PHA (**A**) or VOR (**B**), plated in 12–36 replicate wells depending on the size of the patient's latent reservoir, and cocultured with autologous CD8+ T cells at an E/T ratio of 1:10 in the absence or presence of HIVxCD3 or control DARTs at 100 ng/ml for 24 hours (or up to 96 hours where indicated), after which DARTs were washed off and CD8-depleted PBMCs from a seronegative donor were added to amplify residual virus. Wells were assessed for the presence or absence of p24 by ELISA at day 15. Combo indicates a 1:1 cocktail of 7B2xCD3 and A32xCD3 at a total concentration of 100 ng/ml. Results are shown as percent viral recovery (number of positive wells/total number plated), normalized to a control in which no CD8+ T cells are added. Dashed lines indicate undetectable viral recovery following incubation with combo DARTs, except for patient 408 in panel B, where they indicate undetectable viral recovery after 7B2xCD3 or A32xCD3 individually. NT indicates conditions not tested due to low cell availability. NT generally refers to 2 conditions not tested (7B2xCD3 or A32xCD3 individually), except for patient 408 in panel B, where NT refers to combo DARTs not tested. Refer to Supplemental Table 5 for the individual experimental values for each of the conditions tested.

the control DARTs (Figure 7D). The addition of HIVxCD3 DARTs to a mixture of AR virus–infected CD4+ target cells and autologous CD8+ effector cells led to significantly enhanced reductions in p24 production. At an E/T ratio of 1:10, p24 production was reduced by 0.51 log with 7B2xCD3 ($P < 0.05$), by 0.37 log with A32xCD3, and by 0.79 log with a 1:1 cocktail of the 2 ($P < 0.05$), compared with a reduction of only 0.02 log with CD8+ cells alone (Figure 7E). A trend toward decreased p24 production in the presence of HIVxCD3 DARTs was also seen at the higher E/T ratio of 1:1, although the magnitude of the effect was reduced by the variable baseline CD8+ activity seen in the absence of DARTs (Figure 7F). Notably, ex vivo DART activity was observed with lymphocytes from all 5 patients evaluated with at least one of the 2 HIVxCD3 DARTs and in all cases with the 1:1 DART cocktail.

HIVxCD3 DARTs redirect T cells from HIV-infected individuals on suppressive ART to clear virus from resting CD4+ T cells following induction of latent virus expression. Ultimately, a reagent used in the "shock and kill" HIV eradication strategy must recognize and clear rare infected cells that are likely to express low levels of anti-

gen as they emerge from latency. We therefore employed a latency clearance assay (LCA) as previously described (49). This assay seeks to measure the ability of DARTs to redirect autologous CD8+ T cells to reduce viral recovery following induction of resting CD4+ T cells of HIV-infected individuals on suppressive ART. Addition of fully active DARTs or a 1:1 cocktail of A32xCD3 and 7B2xCD3 to a coculture of CD8+ T cells with PHA-stimulated resting CD4+ T cells at an E/T ratio of 1:10 reduced viral recovery in all 6 patients, although the magnitude of reduction varied among patients (Figure 8A and Supplemental Table 5).

Reversal of HIV latency using maximal mitogen stimulation in vivo is not clinically practical (50). However, the presentation of viral antigen following the reversal of latency with agents that do not result in global T cell activation, such as vorinostat (VOR), may be less robust than that following maximal mitogen stimulation. To evaluate the HIVxCD3 DARTs in a clinically relevant context, we used a physiologically relevant exposure to VOR that models the exposure obtained following a single 400 mg in vivo dose (18) to induce latent viral envelope expression. In this setting, addition

of CD8^{+} T cells at an E/T ratio of 1:10 plus fully active DARTs led to a reduction in viral recovery following a 24-hour coculture period when compared with CD8^{+} T cells with or without control DARTs in 4 of 5 patients tested. In the single patient who did not respond to DARTs after a 24-hour coculture period (patient 795), extending the coculture period from 24 hours to 96 hours led to complete ablation of viral recovery (Figure 8B and Supplemental Table 5).

Discussion

Crucial hurdles in the elimination of the latent HIV-1 reservoir include: (i) the limited ability of the immune system to recognize rare HIV-1–infected cells presenting modest levels of HIV antigen prior to or following induction with LRA (38, 51); (ii) the presence of CD8^{+} cytotoxic T lymphocyte escape mutants in the HIV-1 latent reservoir (52); and (iii) the low frequency of circulating HIV-specific CD8^{+} T cells in patients on ART and the necessity to activate them due to inadequate stimuli provided by infected cells (38). In this study, we present data that HIVxCD3 DARTs could overcome each of these major obstacles.

HIVxCD3 DARTs with HIV arms derived from the nonneutralizing mAbs A32 and 7B2 were able to recognize HIV-1 Env–expressing cell lines and to elicit redirected T cell–killing activity, even when cell-surface Env expression appeared low. In addition, HIVxCD3 DARTs were effective ex vivo in redirecting CD8^{+} T cells to clear resting CD4^{+} T cells obtained from aviremic, ART-treated patients following exposure to VOR.

HIV-1 isolates represented in the latent reservoir are reported to include escape mutants generated by the CD8^{+} T cell responses (52), which may limit the ability of the MHC class I–restricted CD8^{+} CTL responses induced by natural infection to clear HIV-1–infected cells. The A32 and 7B2 arms of the HIVxCD3 DARTs are based on broadly reactive nonneutralizing anti-HIV mAbs that interact with highly conserved residues in gp120 and gp41, respectively, and efficiently mediate ADCC activity against cells infected with HIV-1 isolates of various subtypes. Of note, the A32 mAb epitope is the earliest one known to be expressed on the surface of infected cells during the syncytia formation process (53) or following tier 2 virus infection (54), and the 7B2 mAb epitope is accessible on gp41 stumps, which are expressed on the surface of infected cells during budding and retained at the membrane surface when gp120 subunits dissociate (29, 55). These properties are indicative of the accessibility of the A32 and 7B2 epitopes on the surface of infected cells. Importantly, the existence of CTL escape mutants is not a limitation because CTL epitopes are irrelevant to DART-mediated redirected killing activity. Further, effector T cells recruited by bispecific molecules like DARTs are polyclonal and not MHC-restricted (33). Consistent with these assertions, A32xCD3 and 7B2xCD3 were effective at redirecting CD8^{+} T cells from patients to clear CD4^{+} cells infected by their own AR virus, regardless of the presence of any escape mutations that may have accumulated before initiation of therapy (52). Interestingly, upon in vitro activation of the CD4^{+} T cells used as target cells, we observed a specific reduction in virus recovery in the absence of CD8^{+} T cells, suggesting that DARTs could also recruit cytotoxic CD4^{+} T cells under these particular experimental conditions. In line with these, we found that DARTs induced activation of CD4^{+} T cells in the presence of Env-expressing Jurkat-522 F/Y cells, and

were capable of increasing degranulation of CD4^{+} T cells when cocultured with infected autologous target cells from HIV^{+} individuals. Cytotoxic CD4^{+} T cells have been previously reported in the context of responses to HIV-1 (56) and cytomegalovirus (57). Further studies will be necessary to determine whether effective DART recruitment and redirection of cytotoxic CD4^{+} T cells occurs under in vivo settings.

The relative potencies of the A32xCD3 and 7B2xCD3 DARTs varied among the different test systems employed in our studies, most likely due to variations in the characteristics of the Env-expressing target cells and/or effector T cells. However, whenever one of the DARTs exhibited greater activity than the other, we consistently observed activity similar to that of the more potent DART when combinations of the 2 DARTs were utilized in the studies with infected patients' cells (Figures 7 and 8). Thus, combinations of DARTs targeting different HIV epitopes may be an advantageous strategy to maximize both level and breadth of activity, similar to what has been described for combinations of ADCC-mediating (58) or broadly neutralizing anti–HIV-1 mAbs (59, 60).

Eliminating the pool of latently infected cells by HIV-1–specific CD8^{+} T cell responses is limited by the low frequency of these cells in infected individuals and the need to activate them from the resting state (38). With resting CD8^{+} T cells from HIV-1 seronegative individuals lacking any previous exposure to HIV-1 antigens, HIVxCD3 DARTs induced degranulation of up to 23% of these resting CD8^{+} T cells when incubated with the autologous HIV-1–infected target cells destined to be killed. DARTs were also capable of redirecting CD8^{+} T cells from HIV-1 seropositive individuals who received ART in viral clearance assays. Therefore, HIVxCD3 DART proteins can effectively recruit and redirect CD8^{+} T cytotoxic cells independently of previous exposure to HIV antigens and regardless of any functional impairment that may remain in chronic HIV-1 infection (46, 47, 61).

DART-redirected T cell activity against HIV-1 Env-expressing targets was dependent on HIVxCD3 DART concentration, E/T ratio, and incubation time. The monovalent nature of each of the binding arms of the HIVxCD3 DART molecule ensures that target-cell killing depends exclusively on E/T cell coengagement, as has been observed with CD19xCD3 and other DARTs (31, 32, 34). No HIVxCD3 DART–mediated T cell activation or redirected killing activity was observed in the absence of Env expression on target cells. Similarly, with T cells from HIV-infected patients on suppressive ART, no T cell activation was observed in the absence of virus-infected target cells. Because they should elicit cytotoxic activity from circulating T cells only in the proximity of HIV-1–infected Env-expressing target cells, HIVxCD3 DARTs are not expected to elicit widespread systemic effects, such as inflammatory cytokine release, in HIV-infected patients on ART due to the scarcity of the Env-expressing target cells. The specificity of T cell redirected responses elicited by HIVxCD3 DARTs will be of critical importance clinically, considering that HIV infection induces nonspecific activation of the immune system in both the acute and chronic phases of the disease in HIV-1–specific T cell subsets, as well as in general CD8^{+} T cell populations (62–64).

HIV-infected CD4^{+} T cells expressing cell-surface Env are the primary in vivo targets for HIVxCD3 DART–redirected T cell–killing activity. Because these target cells also express CD3, the

DART molecules could mediate synapses between infected and uninfected CD4+ T cells that, rather than or in addition to redirecting the killing of infected cells, conceivably could facilitate the spread of virus to uninfected cells. However, we did not observe any evidence to suggest that DARTs enhanced the spread of virus, as DARTs reduced p24 production even in the absence of CD8+ T cells (Figure 7, A and D).

In summary, our experiments demonstrate that HIVxCD3 DARTs, with HIV arms derived from the nonneutralizing A32 and 7B2 mAbs, are specific and potent agents to redirect cytolytic T cells against target cells consisting of (i) HIV-1 Env–expressing CD4+ cell lines, (ii) activated CD4+ cells from seronegative individuals infected with HIV-1 IMCs of different subtypes, (iii) activated CD4+ cells from seropositive patients on suppressive ART infected with JR-CSF or AR virus, or (iv) resting CD4+ cells from HIV-infected patients exposed ex vivo to a T cell mitogen (phytohemagglutinin, PHA) or LRA (VOR). Importantly, the studies demonstrated that autologous CD8+ T cells from HIV-infected patients on suppressive ART were efficacious as effector cells in the presence of DARTs. The demonstration of HIVxCD3 DART–mediated T cell–killing activity in the presence of VOR is particularly notable because it provides evidence of activity against authentic latent virus isolates expressed from HIV-infected patients' cells in a model system designed to mimic potential clinical HIV eradication strategies, similar to earlier findings using ex-vivo expanded CTLs (49). Thus, our data indicate that HIVxCD3 DARTs are suitable agents for testing in vivo in combination with LRAs in "shock and kill" HIV eradication strategies.

Methods

IMCs. HIV-1 IMCs for subtype B BaL, subtype AE CM235, and subtype C 1086.C were generated with the backbone derived from NHL4-3 isolate as previously described (65, 66). All IMCs expressed the *Renilla* luciferase reporter gene and preserved all 9 viral open reading frames. The *Renilla* luciferase reporter gene was expressed under the control of the HIV-1 Tat gene. Upon HIV-1 infection of CD4+ T cells, expression of Tat during HIV-1 replication will induce luciferase expression, which allows quantitation of infected cells by measuring relative luminescence units (RLU).

Construction, expression, and purification of HIVxCD3 DARTs. The DARTs were produced from plasmids that coexpressed 2 polypeptide chains: one with light chain variable domain (VL) of anti-CD3 linked to heavy chain variable domain (VH) of anti-HIV and the second with VL of anti-HIV linked to VH of anti-CD3. The carboxy termini of the 2 polypeptide chains consist of paired oppositely charged E-coil/K-coil dimerization domains, which include an interchain disulfide bond (Figure 1). The HIV arm sequences were derived from the nonneutralizing mAbs, A32 (GenBank accession numbers 3TNM_H and 3TNM_L) and 7B2 (GenBank accession numbers AFQ31502 and AFQ31503), and the CD3 arm sequence was derived from hXR32, a humanized mouse anti-human CD3ε mAb (L. Huang, L.S. Johnson, CD3-binding molecules capable of binding to human and nonhuman CD3, US Patent. 20140099318 (2014) (67). Control DARTs were similarly constructed by replacing either the HIV or CD3 specificity with an irrelevant specificity from an anti-fluorescein mAb (4420) (68) or anti-RSV mAb (palivizumab) (69). DART-encoding sequences were cloned into CET1019AD UCOE vectors (EMD Millipore) and trans-

fected into CHO cells, and proteins were purified as described previously (31). Purified proteins were analyzed by SDS-PAGE (NuPAGE Bis-Tris gel system, Invitrogen) and analytical SEC (TSK GS3000S-WxL SE-HPLC, Tosoh Bioscience).

ELISA. For monospecific binding assays, a MaxiSorp microtiter plate (Nunc) coated with recombinant proteins (human CD3ε/δ heterodimer, JR-FL gp140ΔCF; ref. 70) in bicarbonate buffer was blocked with 3% BSA and 0.1% Tween-20. DART proteins were applied, followed by sequential addition of biotinylated anti-EK coil antibody and streptavidin-HRP (BD Biosciences). For bispecific binding assays, the plate was coated with JR-FL gp140ΔCF, and DART application was followed by sequential addition of biotinylated CD3ε/δ and streptavidin-HRP. HRP activity was detected with SuperSignal ELISA Pico chemiluminescent substrate (Thermo Scientific).

SPR analysis. HIVxCD3 DART binding to antigens was analyzed by BIAcore 3000 biosensor (GE Healthcare) as previously described (31, 32). Human CD3ε/δ was immobilized on the CM5 sensor chip according to the manufacturer's procedure. DART binding to immobilized CD3 was analyzed to assess the properties of the CD3 arm, and HIV-1 Env protein binding to HIV DART captured on immobilized CD3 was analyzed to assess the properties of the HIV arm. JR-FL gp140CF was used to assess 7B2xCD3 binding, and M.ConS gp140ΔCFI (70) was used to assess A32xCD3 binding. The different Env proteins were utilized because A32xCD3 did not bind efficiently to JR-FL gp140ΔCF and M.ConS gp140ΔCFI lacks the gp41 binding site for 7B2xCD3. Binding experiments were performed in 10 mM HEPES, pH 7.4, 150 mM NaCl, 3 mM EDTA, and 0.005% P20 surfactant. Regeneration of immobilized receptor surfaces was performed by pulse injection of 10 mM glycine. pH 1.5. K_D values were determined by a global fit of binding curves to the Langmuir 1:1 binding model (BIAevaluation software v4.1).

Cell lines. Jurkat-522 F/Y GF cells, which constitutively express a fusion protein of copepod GFP (copGFP) and firefly luciferase (System Biosciences Inc.), were generated at Macrogenics from Jurkat-522 F/Y cells by transduction and clone selection. HEK293-D371 cells, which have doxycycline-inducible expression of HIV-1 CM244 (subtype AE) gp140, were obtained from John Kappes (University of Alabama at Birmingham, Birmingham, Alabama, USA).

Flow cytometric analysis of DART or mAb binding to cells. DARTs at 4 μg/ml were incubated with 10^5 cells in 200 μl FACS buffer containing 10% human AB serum for 30 minutes at room temperature. After washing, cells were resuspended in 100 μl of 1 μg/ml biotin-conjugated mouse anti-EK antibody (recognizes the E/K heterodimerization region of DART proteins; MacroGenics), mixed with 1:500 diluted streptavidin-PE (BD Biosciences) and incubated in the dark for 45 minutes at 28°C–8°C. Cells were washed, resuspended with FACS buffer, and analyzed with a BD Calibur flow cytometer and FlowJo software (Tree Star Inc.). Binding to IMC-infected CD4+ T cells from normal human donors was conducted as previously described (54) for the A32 and 7B2 mAbs, and with biotin-conjugated mouse anti-EK antibody and 1:500 diluted streptavidin-PE for the HIVx4420 DARTs.

Redirected T cell cytotoxicity assay against HIV-1 Env–expressing cell lines and assessment of T cell activation. Pan T cells were isolated from healthy human PBMCs with the Dynabeads Untouched Human T Cells Kit (Invitrogen). HIV-1 Env–expressing cell lines (1–4 × 10^5 cells/ml) were treated with serial dilutions of DARTs, together with human T cells at an E/T ratio of 10:1, or otherwise

at varying E/T ratios as indicated, and incubated at 37°C, 5% CO_2 overnight. Cytotoxicity was measured by LDH release (CytoTox 96 Non-Radioactive Cytotoxicity Assay, Promega) as described previously (32). With the Jurkat-522 F/Y GF cell line, cytotoxicity was also measured by luminescence using Luciferase-Glo substrate (Promega). Specific lysis was calculated from luminiscence counts (RLU): cytotoxicity (%) = 100 × (1-[RLU of Sample/RLU of Control]), where control equals the average RLU of target cells incubated with effector cells in the absence of DART. Data were fit to a sigmoidal dose-response function to obtain EC_{50} and percent maximum specific lysis values. T cell activation was measured by FACS analysis after cells in the assay plate were labeled with CD8-FITC, CD4-APC, and CD25-PE antibodies (BD Biosciences), followed by cell collection by FACS Calibur flow cytometer equipped with acquisition software CellQuest Pro version 5.2.1 (BD Biosciences). Data analysis was performed using FlowJo software (Tree Star Inc.).

Redirected T cell cytotoxicity assay against HIV-1 IMC–infected CD4+ cells. Cryopreserved resting PBMC from normal healthy HIV-1 seronegative donors were activated for 72 hours with anti–human CD3 (clone OKT3; eBioscience) and anti–human CD28 (clone CD28.2; BD Biosciences). Subsequently, a CD4+ enriched cell population (purity > 92.3%; average ± SD 95.73% ± 2.6%) was obtained by depletion of CD8+ T cells using magnetic beads (Miltenyi Biotec), spinoculated in the presence of the luciferase-expressing IMC-representing HIV-1 subtype AE (CM235), B (BaL), or C (1086.C) and cultured for 72 hours. CD4+-infected target cells were incubated with resting CD8+ effector cells (isolated by negative selection from autologous PBMC, CD8+ T cell Isolation Kit, Miltenyi Biotec) at 33:1, 11:1, 3:1, and 0:1 E/T ratios in the absence or presence of DARTs for 6–48 hours at concentrations ranging from 0.0001–1,000 ng/ml. Uninfected and infected target cells alone were included as additional controls. Each condition was tested in duplicate. After incubation, ViviRen Live Cell Substrate (Promega) was added and RLU was measured on a luminometer; %SL of target cells was determined as described previously (58).

T cell degranulation (CD107) assay. As described for the cytotoxicity assay with HIV-1 IMC–infected cells as targets, activated CD4+ cells infected with HIV-1 BaL IMC were plated with resting CD8+ effector cells at a 33:1 E/T ratio in the absence or presence of 1 ng/ml DARTs and incubated for 6 hours. For the CD4+ T cell degranulation, activated CD4+ T cells were either infected with JR-CSF and labeled with the viability (NFL1) and target-specific (TFL4) markers routinely utilized in our ADCC assay (71) or added to targets as effectors at a 10:1 ratio prior to addition of DARTs. Each condition was tested in duplicate. CD107 PE-Cy5 (clone H4A3; eBioscience) was titered and added during the last 6 hours of the incubation, along with Monensin solution (BD Biosciences) (72). A panel of antibodies consisting of LIVE/DEAD Aqua stain, anti–CD3 APC-H7 (clone SK7; BD Biosciences), anti–CD4 BV605 (clone OKT4; BioLegend), and anti–CD8 BV650 (clone RPA-T8; BioLegend) was used to detect CD107+ CD8+ T cells. After washing and fixation, samples were acquired on a custom-made LSRII (BD Bioscience) within the next 24 hours. A minimum of 300,000 total viable events was acquired for each test. The analysis of the data was performed using the Flow-Jo software (Tree Star Inc.).

T cell viability and activation assays. CD8+ T cells and CD8-depleted PBMCs obtained from HIV-infected, ART-suppressed patients were plated at $5 × 10^4$ cells per well in 96-well plates with 100 ng/ml of the indicated DART. Cells were cultured in 0.2 ml of cIMDM media supplemented with 10% FBS, 1% Penicillin/Streptomycin, and 5 U/ml IL-2 for 7 days, and then stained with the following antibodies: HLA-DR-PerCP (clone L243), CD25-PE (clone M-A251), CD8-FITC (clone HIT8a), CD8-PE (clone HIT8a), CD4-FITC (clone RPA-T4), Annexin V-PE, and 7-AAD (all BD Biosciences).

Redirected T cell viral clearance assay. CD8+ T cells were isolated from PBMCs by positive selection (EasySep human CD8+ Selection Kit, StemCell Technologies Inc.). CD8-depleted PBMCs were first activated with 2 μg/ml of PHA (Remel and Lenexa, Kansas, USA) and 60 U/ml of IL-2, and then infected by spinoculation at 1,200 × g for 90 minutes with either JR-CSF or AR virus at an MOI of 0.01 as previously described (49). AR virus was obtained from pooled supernatants of replicate wells from outgrowth assays of resting CD4+ T cells for each patient performed as previously described (73). Fifty-thousand ($5 × 10^4$) targets/well were cocultured with CD8+ T cells in triplicate at the indicated E/T ratio in the absence or presence of 100 ng/ml of DART in 0.2 m of cIMDM media supplemented with 10% FBS, 1% Penicillin/Streptomycin, and 5 U/ml IL-2 . For experiments performed in the presence of ARVs, 24 hours after spinoculation cells were washed and 1 μM of raltegravir and 4 μM of abacavir were added, and then DARTs and CD8+ T cells were added to cultures. Supernatant was assayed on day 7 by p24 ELISA (ABL). Results are calculated as the log fold reduction (log of [p24 levels of infected target cells divided by p24 levels of the test condition]).

LCA. We assessed the reduction of virus recovery from CD4+-infected cells by a standard quantitative viral outgrowth assay using the resting CD4+ T cells of aviremic, ART-treated patients, following the addition of antiviral effector cells and/or molecules as previously described (49). In this case, we used the LCA to model the ability of DARTs to clear virus emerging from the latent reservoir under clinically and pharmacologically relevant conditions. Resting CD4+ T cells were isolated from a leukapheresis product as previously described (73) and either exposed to PHA (4 μg/ml) and IL-2 (60 U/ml) for 24 hours or VOR (335 nM, 6 hours) (Merck), and plated at 0.5 to $1 × 10^6$ cells/well in 12–36 replicate wells, depending on the size of the reservoir. The VOR was then washed off and CD8+ T cells added at an E/T of 1:10, along with 100 ng/ml of the indicated DART. Cells were cocultured for 24 hours (unless specified otherwise) following which the DART proteins were washed off and allogeneic CD8-depleted PBMCs from an HIV-1 seronegative donor were added to amplify residual virus. Supernatant was assayed for the presence of p24 antigen on day 15 for each well. Results are calculated as percent viral recovery ([number of positive wells/total number plated] × 100), normalized to a control in which no CD8+ T cells are added.

Patient population. Leukapheresis samples were obtained from HIV seronegative donors or HIV-infected donors with undetectable plasma viremia (<50 copies/ml) on stable ART for at least 6 months, as indicated. Written informed consent was obtained from each patient, and the study was approved by the Duke and UNC Biomedical Institutional Review Boards.

Statistics. Statistical comparisons between groups were analyzed using the Dunnett's test for multiple comparisons using GraphPad Prism Software; P values <0.05, calculated with Dunnett correction for multiple comparisons, were considered significant.

Address correspondence to: David M. Margolis, 120 Mason Farm Road, GMB CB #7042, Chapel Hill, North Carolina, USA. Phone: 919.966.6389; E-mail: david_margolis@med.unc.edu. OR to: Guido Ferrari, Duke University Medical Center, Department of Surgery, P.O. Box 2926, Durham, North Carolina, 27710, USA. Phone: 919.684.2862; E-mail: gflmp@dm.duke.edu.

1. Chun TW, Finzi D, Margolick J, Chadwick K, Schwartz D, Siliciano RF. In vivo fate of HIV-1-infected T cells: quantitative analysis of the transition to stable latency. *Nat Med*. 1995;1(12):1284–1290.

2. Chun TW, et al. Quantification of latent tissue reservoirs and total body viral load in HIV-1 infection. *Nature*. 1997;387(6629):183–188.

3. Finzi D, et al. Identification of a reservoir for HIV-1 in patients on highly active antiretroviral therapy. *Science*. 1997;278(5341):1295–1300.

4. Wong JK, et al. Recovery of replication-competent HIV despite prolonged suppression of plasma viremia. *Science*. 1997;278(5341):1291–1295.

5. Pierson TC, Zhou Y, Kieffer TL, Ruff CT, Buck C, Siliciano RF. Molecular characterization of preintegration latency in human immunodeficiency virus type 1 infection. *J Virol*. 2002;76(17):8518–8531.

6. Pomerantz RJ. Reservoirs of human immunodeficiency virus type 1: the main obstacles to viral eradication. *Clin Infect Dis*. 2002;34(1):91–97.

7. Chomont N, et al. HIV reservoir size and persistence are driven by T cell survival and homeostatic proliferation. *Nat Med*. 2009;15(8):893–900.

8. Bosque A, Famiglietti M, Weyrich AS, Goulston C, Planelles V. Homeostatic proliferation fails to efficiently reactivate HIV-1 latently infected central memory CD4+ T cells. *PLoS Pathog*. 2011;7(10):e1002288.

9. Soriano-Sarabia N, et al. Quantitation of replication-competent HIV-1 in populations of resting CD4+ T cells. *J Virol*. 2014;88(24):14070–14077.

10. Palmer S, et al. New real-time reverse transcriptase-initiated PCR assay with single-copy sensitivity for human immunodeficiency virus type 1 RNA in plasma. *J Clin Microbiol*. 2003;41(10):4531–4536.

11. Palmer S, et al. Low-level viremia persists for at least 7 years in patients on suppressive antiretroviral therapy. *Proc Natl Acad Sci U S A*. 2008;105(10):3879–3884.

12. Dinoso JB, et al. Treatment intensification does not reduce residual HIV-1 viremia in patients on highly active antiretroviral therapy. *Proc Natl Acad Sci U S A*. 2009;106(23):9403–9408.

13. Gandhi RT, et al. No evidence for decay of the latent reservoir in HIV-1–infected patients receiving intensive enfuvirtide-containing antiretroviral therapy. *J Infect Dis*. 2010;201(2):293–296.

14. Davey RT Jr, et al. HIV-1 and T cell dynamics after interruption of highly active antiretroviral therapy (HAART) in patients with a history of sustained viral suppression. *Proc Natl Acad Sci U S A*. 1999;96(26):15109–15114.

15. Carcelain G, et al. Transient mobilization of human immunodeficiency virus (HIV)-specific CD4 T-helper cells fails to control virus rebounds during intermittent antiretroviral therapy in chronic HIV type 1 infection. *J Virol*. 2001;75(1):234–241.

16. Rothenberger MK, et al. Large number of rebounding/founder HIV variants emerge from multifocal infection in lymphatic tissues after treatment interruption. *Proc Natl Acad Sci U S A*. 2015;112(10):E1126–E1134.

17. Robb ML, Kim JH. Shot in the HAART: vaccine therapy for HIV. *Lancet Infect Dis*. 2014;14(4):259–260.

18. Archin NM, et al. Administration of vorinostat disrupts HIV-1 latency in patients on antiretroviral therapy. *Nature*. 2012;487(7408):482–485.

19. Denton PW, et al. Targeted cytotoxic therapy kills persisting HIV infected cells during ART. *PLoS Pathog*. 2014;10(1):e1003872.

20. Ho YC, et al. Replication-competent noninduced proviruses in the latent reservoir increase barrier to HIV-1 cure. *Cell*. 2013;155(3):540–551.

21. Bullen CK, Laird GM, Durand CM, Siliciano JD, Siliciano RF. New ex vivo approaches distinguish effective and ineffective single agents for reversing HIV-1 latency in vivo. *Nat Med*. 2014;20(4):425–429.

22. Cillo AR, et al. Quantification of HIV-1 latency reversal in resting CD4+ T cells from patients on suppressive antiretroviral therapy. *Proc Natl Acad Sci U S A*. 2014;111(19):7078–7083.

23. Pincus SH. Therapeutic potential of anti-HIV immunotoxins. *Antiviral Res*. 1996;33(1):1–9.

24. Davey RT Jr, et al. Use of recombinant soluble CD4 Pseudomonas exotoxin, a novel immunotoxin, for treatment of persons infected with human immunodeficiency virus. *J Infect Dis*. 1994;170(5):1180–1188.

25. Bera TK, Kennedy PE, Berger EA, Barbas CFI, Pastan I. Specific killing of HIV-infected lymphocytes by a recombinant immunotoxin directed against the HIV-1 envelope glycoprotein. *Mol Med*. 1998;4(6):384.

26. Denton PW, et al. Generation of HIV latency in humanized BLT mice. *J Virol*. 2012;86(1):630–634.

27. Pollara J, Bonsignori M, Moody MA, Pazgier M, Haynes BF, Ferrari G. Epitope specificity of human immunodeficiency virus-1 antibody dependent cellular cytotoxicity [ADCC] responses. *Curr HIV Res*. 2013;11(8):378–387.

28. Acharya P, et al. Structural definition of an antibody-dependent cellular cytotoxicity response implicated in reduced risk for HIV-1 infection. *J Virol*. 2014;88(21):12895–12906.

29. Pincus SH, Fang H, Wilkinson RA, Marcotte TK, Robinson JE, Olson WC. In vivo efficacy of anti-glycoprotein 41, but not anti-glycoprotein 120, immunotoxins in a mouse model of HIV infection. *J Immunol*. 2003;170(4):2236–2241.

30. Craig RB, Summa CM, Corti M, Pincus SH. Anti-HIV double variable domain immunoglobulins binding both gp41 and gp120 for targeted delivery of immunoconjugates. *PLoS One*. 2012;7(10):e46778.

31. Johnson S, et al. Effector cell recruitment with novel Fv-based dual-affinity re-targeting protein leads to potent tumor cytolysis and in vivo B-cell depletion. *J Mol Biol*. 2010;399(3):436–449.

32. Moore PA, et al. Application of dual affinity retargeting molecules to achieve optimal redirected T-cell killing of B-cell lymphoma. *Blood*. 2011;117(17):4542–4551.

33. Nagorsen D, Baeuerle PA. Immunomodulatory therapy of cancer with T cell-engaging BiTE antibody blinatumomab. *Exp Cell Res*. 2011;317(9):1255–1260.

34. Chichili GR, et al. A CD3xCD123 bispecific DART for redirecting host T cells to myelogenous leukemia: preclinical activity and safety in nonhuman primates. *Sci Transl Med*. 2015;7(289):289ra82.

35. Topp MS, et al. Phase II trial of the anti-CD19 bispecific T cell-engager blinatumomab shows hematologic and molecular remissions in patients with relapsed or refractory B-precursor acute lymphoblastic leukemia. *J Clin Oncol*. 2014;32(36):4134–4140.

36. Topp MS, et al. Safety and activity of blinatumomab for adult patients with relapsed or refractory B-precursor acute lymphoblastic leukaemia: a multicentre, single-arm, phase 2 study. *Lancet Oncol*. 2014;16(1):57–66.

37. Rader C. DARTs take aim at BiTEs. *Blood*. 2011;117(17):4403–4404.

38. Shan L, et al. Stimulation of HIV-1–specific cytolytic T lymphocytes facilitates elimination of latent viral reservoir after virus reactivation. *Immunity*. 2012;36(3):491–501.

39. Moore JP, et al. Exploration of antigenic variation in gp120 from clades A through F of human immunodeficiency virus type 1 by using monoclonal antibodies. *J Virol*. 1994;68(12):8350–8364.

40. Guan Y, et al. Diverse specificity and effector function among human antibodies to HIV-1 envelope glycoprotein epitopes exposed by CD4 binding. *Proc Natl Acad Sci U S A*. 2013;110(1):E69–78.

41. Veillette M, et al. Interaction with cellular CD4 exposes HIV-1 envelope epitopes targeted by antibody-dependent cell-mediated cytotoxicity. *J Virol*. 2014;88(5):2633–2644.

42. Zhang MY, et al. Identification and characterization of a broadly cross-reactive HIV-1 human monoclonal antibody that binds to both gp120 and gp41. *PLoS One*. 2012;7(9):e44241.

43. Wyatt R, Moore J, Accola M, Desjardin E, Robinson J, Sodroski J. Involvement of the V1/V2 variable loop structure in the exposure of human immunodeficiency virus type 1 gp120 epitopes induced by receptor binding. *J Virol*. 1995;69(9):5723–5733.

44. Sanders RW, et al. A next-generation cleaved, soluble HIV-1 Env Trimer, BG505 SOSIP.664 gp140, expresses multiple epitopes for broadly neutralizing but not non-neutralizing antibodies. *PLoS Pathog*. 2013;9(9):e1003618.

45. Cao J, Park IW, Cooper A, Sodroski J. Molecular determinants of acute single-cell lysis by human immunodeficiency virus type 1. *J Virol*. 1996;70(3):1340–1354.

46. Trautmann L, Janbazian L, Chomont N, Said E. Upregulation of PD-1 expression on HIV-specific CD8 T cells leads to reversible immune dysfunction. *Nat Med*. 2006;12(10):1198–1202.

47. Blackburn SD, et al. Coregulation of CD8+ T cell exhaustion by multiple inhibitory receptors during chronic viral infection. *Nat Immunol*. 2008;10(1):29–37.

48. Groux H, Torpier G, Monté D, Mouton Y, Capron A, Ameisen JC. Activation-induced death by apoptosis in CD4+ T cells from human immunodeficiency virus-infected asymptomatic individuals. *J Exp Med*. 1992;175(2):331–340.

49. Sung JA, et al. Expanded cytotoxic T-cell lymphocytes target the latent HIV reservoir. *J Infect Dis*. 2015;212(2):1–15.

50. van Praag RM, et al. OKT3 and IL-2 treatment for purging of the latent HIV-1 reservoir in vivo results in selective long-lasting CD4+ T cell depletion. *J Clin Immunol*. 2001;21(3):218–226.

51. Durand CM, Blankson JN, Siliciano RF. Developing strategies for HIV-1 eradication. *Trends Immunol*. 2012;33(11):554–562.

52. Deng K, et al. Broad CTL response is required to clear latent HIV-1 due to dominance of escape mutations. *Nature*. 2015;517(7534):381–385.

53. Finnegan CM, Berg W, Lewis GK, DeVico AL. Antigenic properties of the human immunodeficiency virus envelope during cell-cell fusion. *J Virol*. 2001;75(22):11096–11105.

54. Ferrari G, et al. An HIV-1 gp120 envelope human monoclonal antibody that recognizes a C1 conformational epitope mediates potent antibody-dependent cellular cytotoxicity (ADCC) activity and defines a common ADCC epitope in human HIV-1 serum. *J Virol*. 2011;85(14):7029–7036.

55. Moore PL, et al. Nature of nonfunctional envelope proteins on the surface of human immunodeficiency virus type 1. *J Virol*. 2006;80(5):2515–2528.

56. Johnson S, et al. Cooperativity of HIV-specific cytolytic CD4 T cells and CD8 T cells in control of HIV viremia. *J Virol*. 2015;89(15):7494–7505.

57. Casazza JP, et al. Acquisition of direct antiviral effector functions by CMV-specific CD4+ T lymphocytes with cellular maturation. *J Exp Med*. 2006;203(13):2865–2877.

58. Pollara J, et al. HIV-1 vaccine-induced C1 and V2 Env-specific antibodies synergize for increased antiviral activities. *J Virol*. 2014;88(14):7715–7726.

59. Shingai M, et al. Antibody-mediated immunotherapy of macaques chronically infected with SHIV suppresses viraemia. *Nature*. 2013;503(7475):277–280.

60. Barouch DH, et al. Therapeutic efficacy of potent neutralizing HIV-1-specific monoclonal antibodies in SHIV-infected rhesus monkeys. *Nature*. 2013;503(7475):224–228.

61. Yamamoto T, et al. Surface expression patterns of negative regulatory molecules identify determinants of virus-specific CD8+ T-cell exhaustion in HIV infection. *Blood*. 2011;117(18):4805–4815.

62. Giorgi JV, Liu Z, Hultin LE, Cumberland WG, Hennessey K, Detels R. Elevated levels of CD38+ CD8+ T cells in HIV infection add to the prognostic value of low CD4+ T cell levels: results of 6 years of follow-up. The Los Angeles Center, Multicenter AIDS Cohort Study. *J Acquir Immune Defic Syndr*. 1993;6(8):904–912.

63. Perfetto SP, et al. CD38 expression on cryopreserved CD8+ T cells predicts HIV disease progression. *Cytometry*. 1998;33(2):133–137.

64. Vinikoor MJ, et al. Antiretroviral therapy initiated during acute HIV infection fails to prevent persistent T-cell activation. *J Acquir Immune Defic Syndr*. 2013;62(5):505–508.

65. Edmonds TG, et al. Replication competent molecular clones of HIV-1 expressing Renilla luciferase facilitate the analysis of antibody inhibition in PBMC. *Virology*. 2010;408(1):1–13.

66. Adachi A, et al. Production of acquired immunodeficiency syndrome-associated retrovirus in human and nonhuman cells transfected with an infectious molecular clone. *J Virol*. 1986;59(2):284–291.

67. Huang L, Johnson LS, inventors; Macrogenics, Inc., assignee. CD3-binding molecules capable of binding to human non-human CD3. US patent US20140099318 A1. April 10, 2014.

68. Kranz DM, Voss EW. Partial elucidation of an anti-hapten repertoire in BALB/c mice: comparative characterization of several monoclonal anti-fluorescyl antibodies. *Mol Immunol*. 1981;18(10):889–898.

69. Johnson S, et al. Development of a humanized monoclonal antibody (MEDI-493) with potent in vitro and in vivo activity against respiratory syncytial virus. *J Infect Dis*. 1997;176(5):1215–1224.

70. Liao HX, et al. A group M consensus envelope glycoprotein induces antibodies that neutralize subsets of subtype B and C HIV-1 primary viruses. *Virology*. 2006;353(2):268–282.

71. Pollara J, et al. High-throughput quantitative analysis of HIV-1 and SIV-specific ADCC-mediating antibody responses. *Cytometry A*. 2011;79(8):603–612.

72. Betts MR, et al. Sensitive and viable identification of antigen-specific CD8+ T cells by a flow cytometric assay for degranulation. *J Immunol Methods*. 2003;281(1–2):65–78.

73. Archin NM, et al. Valproic acid without intensified antiviral therapy has limited impact on persistent HIV infection of resting CD4+ T cells. *AIDS*. 2008;22(10):1131–1135.